Chem. Res. Chinese Universities, 2019, 35(3), 521—529 doi: 10.1007/s40242-019-8341-0

# *In-situ* Synthesis and Characterization of Poly(vinyl alcohol)/ Hydroxyapatite Composite Hydrogel by Freezing-thawing Method

MENG Deyue[1], ZHOU Xiuqing[1], ZHENG Keyan[1], MIAO Chong[2], SHENG Ye[1*] and ZOU Haifeng[1*]

*1. College of Chemistry, Jilin University, Changchun 130012, P. R. China;*
*2. JA Biotech Co., Ltd., Changchun 130103, P. R. China*

**Abstract** Poly(vinyl alcohol)/hydroxyapatite(PVA/HA) composite hydrogel was successfully *in-situ* synthesized *via* three cycles of freezing-thawing. The composition and structure of products were investigated by X-ray diffraction(XRD), Fourier transformed infrared spectroscopy(FTIR) and scanning electron microscopy(SEM). The influence of different preparation methods and contents of material on the mechanical properties of PVA/HA composite hydrogel was discussed through tensile and compressive tests. The template of PVA could avoid the agglomeration of HA particles, which improves the mechanical properties of the composite hydrogel effectively. The tensile strength, modulus and compressive performances of the PVA/HA composite hydrogel prepared by the *in-situ* synthesis method were better than those of hydrogel obtained by the simple blend method. In addition, the effect of the content of PVA, HA, and the pH value on the properties of the PVA/HA composite hydrogel has been discussed in detail.

**Keywords** Composite hydrogel; *In-situ* synthesis; Tensile property; Compressive property

## 1 Introduction

As a hydrophilic material with a special network structure, hydrogel has received wide attention over the past decades. In many kinds of hydrogels, poly(vinyl alcohol)(PVA) hydrogel possesses available pendant alcohol groups that can serve as attachment points for biological molecules, having some level of permeability, biodegradability, and excellent biocompatibility. The elastic nature of the hydrogel can induce cell orientation or matrix synthesis by enhancing the transmission of mechanical stimuli to seeded cells[1]. Within a number of polymers capable of forming hydrogels, PVA has shown permissible as implants[2] because of its microporous structures, no side effects, non-toxic and chemically stable[3,4]. Based on the PVA matrix, numerous scholars have done a great deal study on the bone tissue regeneration, implantable artificial organelles, cardiovascular tissue, artificial cornea, skin wound, articular cartilage tissue and so on[5—7].

However, the major challenge of PVA hydrogel used in clinical application is its insufficient surface activity and mechanical strength. At present, the PVA hydrogel is usually modified by introducing additional components, such as chemical agents, nanoparticles, biomolecules, natural polymer and synthetic polymer[8]. It is worth mentioning that the PVA hydrogel can be endowed with unique properties after compositing with inorganic nanoparticles[9,10]. Hydroxyapatite(HA), a mineral of calcium phosphate used as biological material, can be found in the teeth and bones of animals widely. And it has been applied diffusely in medical field as a bone repair material due to its brilliant bioactive properties[11]. Adding HA to PVA hydrogel can improve the mechanical properties of hydrogels and provide the biological surface activity. Xu *et al*.[12] reported the blend preparation method of *n*-HA /PVA-H composite hydrogels: *n*-HA and PVA composite solutions were exposed to freezing at –20 °C and thawing at room temperature, repeated several times and formed composite hydrogel. However, the simple physical blend cannot control the morphology of materials and initiate the interfacial chemical reactions between organic and inorganic phases. Maiolo *et al*.[13] prepared PVA/HA composite hydrogels by *in-situ* crosslinking method and repeated freezing-thawing. With the increase of the content of HA, there were no significant changes in the composite hydrogels' glass transition temperature, the melting point and structural water content. The uniform distribution of HA in the PVA matrix has a direct positive impact on mechanical properties of hydrogels. Similarly, PVA/HA composite materials were prepared using $Ca(NO_3)_2$, $(NH_4)_2HPO_4$, and PVA as materials by *in-situ* synthesis by Li *et al*.[14]. They pointed out that the increasing contents of PVA and HA could both improve the compression resistance of the hydrogels. Similar to the responses to external stress of natural articular cartilage, the composite material was expected to be applied in the area of

*Corresponding authors. Email: shengye@jlu.edu.cn; haifengzou0431@sohu.com

Received October 23, 2018; accepted January 3, 2019.

Supported by the Science and Technology Development Plan of Changchun, China(No.17DY019) and the Cooperative Project of Changchun JA Biotech Co., Ltd. and Jilin University, China(No.3R116W751412).

cartilage repair. In these *in-situ* synthesis methods, investigators usually prepared PVA/HA composite materials under the condition of pH values of 9—11[15,16]. The reason is that the high pH value can contribute to the formation of single HA phase and the acceleration of the nucleation, resulting in the formation of fine grains[17]. Furthermore, the pH around 9—10 is an optimum value for the best interaction between PVA and HA[18]. However, the high pH value is unfavorable for biological applications.

In this paper, we prepared PVA/HA hydrogel by *in-situ* synthesis method combining with the molding process of cyclic freezing/thawing(F/T) technique. Meanwhile, PVA/HA hydrogel has also been prepared by simple blend method combined with the cyclic F/T according to the literature for comparison[19]. The effect of two preparation methods on the properties of the composite materials was investigated. In addition, the influence of the PVA and HA contents on structure and mechanical properties of composite materials in the process of *in-situ* synthesis was also discussed in detail. Furthermore, in order to improve its property, the pH value of the system was adjusted to 10 to ensure that the HA could grow and distribute uniformly, and then the pH was adjusted to about 7 before cyclic F/T to make it much more favorable for biological applications. The impact of pH value on the performance of composite materials was also investigated.

# 2 Experimental

## 2.1 Materials

PVA was from Aladdin(polymerization degree: 1700, alcoholysis degree: 87.0%—89.0%); CaO(A. R., 98%, Changzhou Branch Chemical Reagent Co., Ltd.); $H_3PO_4$(A. R., 85%, Beijing Chemical Works); NaOH(A. R., 96%, Beijing Chemical Works). The chemicals were used without further purification. Distilled water was used as a solvent in all experiments.

## 2.2 Preparation of PVA/HA Composite Hydrogels

PVA/HA composite hydrogels were prepared by *in-situ* synthesis and blend method, respectively. For *in-situ* synthesis, firstly, boiling water was added to the necessary amounts of CaO, sealed and aged for 12 h to form $Ca(OH)_2$ slurry. Secondly, a certain amount of PVA was dissolved in $Ca(OH)_2$ solution and then agitated intensively until homogeneously mixed. Afterwards, according to the theoretical HA stoichiometric ratio of Ca/P=1.67, the required amount of $H_3PO_4$ was added, stirred to make sure mixing evenly. Then NaOH solution (10 mol/L) was added to adjust pH value to 10 under continuous stirring, and persisting for 4 h, formed uniform PVA/HA mixture. For comparison, the pH value was also adjusted to 7 through adding $H_3PO_4$ dropwise. PVA aqueous solution with pH value of 10 followed the same steps without the addition of CaO and $H_3PO_4$.

For comparison, PVA/HA composite hydrogel was also prepared by simple blend method. Namely, firstly, HA was prepared by precipitation method. Same as *in-situ* synthesis, without adding PVA, HA suspension was obtained after aging, reaction and pH adjustment. After ageing for 12 h at room temperature, the precipitation was filtrated and washed with deionized water. The white HA powders were obtained after drying at 60 °C for 12 h. Secondly, the 2%(mass fraction) HA powder was thoroughly grounded and added to the aqueous solution, stirred enough until homogeneously mixed. And then 8%(mass fraction) PVA powder was added to the HA aqueous solution, mixed evenly at 95 °C and stirred for 4 h. PVA/HA mixed solution was formed.

Finally, the uniform PVA aqueous solution and PVA/HA mixture were allowed to cool at room temperature and placed in an ultrasonic bath for 30 min to remove trapped air. The final hydrogels were prepared by three cyclic of freezing/thawing (F/T, freezing at −30 °C for 9 h and thawing at 30 °C for 3 h).

## 2.3 Characterization

The crystal structure of HA, PVA hydrogel and PVA/HA composite hydrogel were determined by X-ray diffraction(XRD) on a Rigaku D/max-RA X-ray diffractometer(Rigaku Corporation, Japan) using Cu $K\alpha$ radiation($\lambda$=0.15406 nm) and Ni filter. The major functional groups of the samples were obtained using a Perkin-Elmer 580B infrared spectrophotometer(FTIR). The microstructures of HA and hydrogels were analyzed using the field emission electron microscope(SEM, S-4800, Hitachi Limited, Japan) with an accelerating voltage of 3 kV. The elemental analysis was obtained by energy-dispersive X-ray(EDX, JEOL, Japan) with an HJEOL JXA-840 EDX system attached to the SEM microscope.

The samples were dried to a constant mass, and the rate of quality changes before and after drying were recorded as water content. Water absorption was carried out in distilled water. All samples were dried before immersion at 60 °C for 24 h and then the change of quality with time was recorded to get the water absorption.

Tensile and compression tests were done by using 2 kN load cell in a Universal Table-top Mechanical testing machine.

Tensile stress($\sigma_t$) was calculated as follows:

$$\sigma_t=F/A \quad (1)$$

where $F$(*N*) is the force acting on the section of the sample; $A$($m^2$) represents the cross-sectional area of the narrow section of the sample. Tensile strain($\varepsilon_t$) is defined as the increment of the original standard distance unit length. Tensile strength($\sigma_T$) and elongation($\varepsilon_T$) of a specimen are the tensile stress and strain when the specimens were broken. Stress and strain between $\varepsilon$=10% and 30% were used to calculate the elastic modulus($E_T$), the elastic modulus is the ratio of stress and strain:

$$E_T=\sigma_t/\varepsilon_t \quad (2)$$

Compressive stress can be calculated by

$$\sigma_c=4F/\pi d^2 \quad (3)$$

where $F$(*N*) is the force acting on the section of the sample and $d$(m) is the diameter of the section of the sample. The compressive stress with the compressive strain ratio at 60% was designated as the compressive strength($\sigma_c$). Compressive modulus is the ratio of stress to strain:

$$E_c=\Delta\sigma_c/\Delta\varepsilon_c \quad (4)$$

The value of $\Delta\varepsilon_c$ is 1% and $\Delta\sigma_c$ is the change of stress in this range. Three specimens were tested and average compressive strength and modulus were calculated.

## 3 Results and Discussion

### 3.1 Structural Characterization and Effect of Synthesis Routes on PVA/HA Composite Hydrogel

The XRD patterns of the products are shown in Fig.1. As it can be observed, the good match between standard(JCPDS No. 09-0432) and HA samples(Fig.1 curve *a*) indicates high phase-purity of the as-obtained HA samples[20]. Fig.1 curve *b* reveals the PVA polymer is a semi-crystalline structure with a large peak at $2\theta$=19°—20° and a smaller diffraction peak at around 41°[21,22]. PVA is a semicrystalline polymer, and PVA crystallites act as the cross-linking points in common PVA hydrogels prepared with the cyclic F/T method. The XRD patterns of PVA/HA composite hydrogel(Fig.1 curves *c* and *d*) include the characteristic peaks of both HA and PVA, which proved that HA has been synthesized in PVA solution by the two synthesis routes. However, it is not difficult to find that the HA's diffraction peaks in Fig.1 curve *d* are wider than those in Fig.1 curve *c*, proving that the grain size of HA formed by *in-situ* synthesis is smaller than that of HA prepared by blending method.

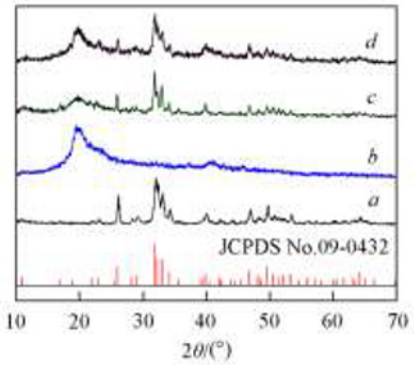


**Fig.1 XRD patterns of HA(*a*), PVA hydrogel(*b*) and PVA/HA composite hydrogels prepared by blend method(*c*) and *in-situ* method(*d*)**

Fig.2 shows the SEM images of HA, PVA hydrogel, and PVA/HA composite hydrogels. It can be seen that the synthesized HA samples exhibit irregularly shaped nano-sized particles. PVA hydrogel contains lots of micro holes with different pore sizes and thicker skeleton. A large number of hydroxyl groups on the molecular chain of PVA form intra- and inter-hydrogen bonding under cyclic F/T, leading to the fabrication of a micro-pore structure[23]. It is beneficial to the growth of chondrocytes as artificial cartilage repairing material[24,25]. The introduction of HA changed the microstructure of PVA hydrogel dramatically. The composite hydrogel prepared by blend method shows the merger of PVA and HA. The clusters in composite hydrogels can be distinguished[Fig.2(C)]. PVA/HA composite hydrogel compounded by *in-situ* synthesis method presents a porous network structure, accompanied by the HA particles distributed in the PVA matrix uniformly. The networks interpenetrate each other with different sizes of holes. In the synthesis process, there is an interaction between the two substrates, impelling morphology to change obviously, especially in the process of *in-situ* synthesis. The PVA molecular chain could be used as a template, which $Ca^{2+}$ was attracted and held by Coulomb forces to ensure that $PO_4^{3-}$ could be combined with $Ca^{2+}$, initiating the nucleation of HA, followed by the growth of HA particles in the PVA matrix[14]. From Fig.2, it can be concluded that the *in-situ* synthesis method is more helpful for the formation of three-dimensional network structure and the dispersion of HA nano-particles.

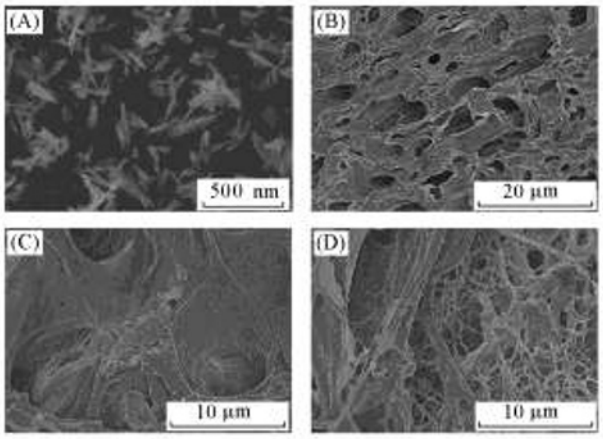


**Fig.2 SEM images of HA(A), PVA hydrogel(B), and PVA/HA composite hydrogels prepared by blend method(C) and *in-situ* method(D)**

To prove the presence of interaction force between HA and PVA, FTIR characterization of HA, PVA, and PVA/HA composite hydrogel was performed. In the FTIR spectrum of HA(Fig.3 curve *a*), the stretching vibration of P—O functional groups results in the absorbance peak at 1026 $cm^{-1}$. In addition, the peaks at 604 and 566 $cm^{-1}$ are attributed to the flexural vibrations of P—O bond[26]. In the spectrum of PVA hydrogel (Fig.3 curve *b*), the peak at 3740 $cm^{-1}$ is an indicative of free alcoholic hydroxyl. The broad and strong absorption band at 3600—3000 $cm^{-1}$ is due to the existence of hydrogen bonded alcoholic hydroxyl groups. The peaks at 2941 and 2916 $cm^{-1}$ are assigned as C—H stretching vibration and the peak at

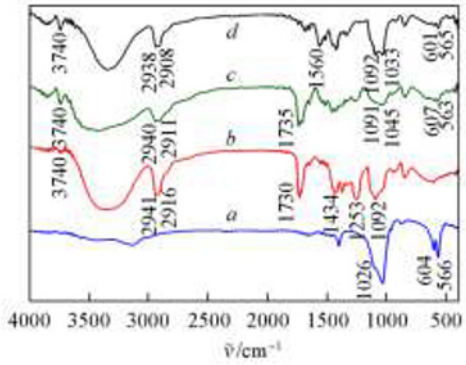


**Fig.3 FTIR spectra of HA(*a*), PVA hydrogel(*b*), and PVA/HA composite hydrogels prepared by blend method(*c*) and *in-situ* method(*d*)**

1434 $cm^{-1}$ indicates the in-plane bending vibration of C—H. The absorption band at 1730 $cm^{-1}$ is attributed to the carbonyl groups from non-hydrolyzed acetate groups when PVA was produced. The peak at 1253 $cm^{-1}$ represents C—C stretching[27,28]. It is noteworthy that there is a stretching vibration peak at 1092 $cm^{-1}$ in the absorption curve, which belongs to the C—O functional groups. Such a vibrational band has been used to prove that PVA is a semicrystalline structure according to the literature[29]. From Fig.3 curves *c* and *d*, it can be observed that the vibration bands of each functional group in HA and PVA molecule have been recurred in the spectra of the PVA/HA composites. However, the positions of the peaks are a little right-shift, especially in the Fig.3 curve *d*, while for Fig.3 curve *c*, the positions do not change significantly. It is well-known that the formation of intra- or intermolecular forces can lower the force constants of the chemical bonds, therefore their vibrational frequencies are shifted to lower wavenumbers[12,30]. This result shows that there are strong hydrogen bonds between PVA molecules, PVA and HA molecules in the process of *in-situ* and cyclic F/T synthesis. In addition, for Fig.3 curve *d*, the broad absorption band at 3600—3000 $cm^{-1}$ becomes narrower, which is also caused by stronger hydrogen bond. Compared to PVA hydrogel, the characteristic absorption peak of 1730 $cm^{-1}$ disappears and a new strong absorption peak emerges at 1560 $cm^{-1}$ after adding HA through *in-situ* synthesis. This may be due to the saponification of PVA under alkaline conditions[31], at the same time, carboxylate salt is formed in the system[32].

As shown in Fig.4, the tensile and compressive properties of PVA/HA composite hydrogel prepared by *in-situ* method are better than those prepared by blend method. The tensile strength($\sigma_T$) and elastic modulus($E_T$) are doubled, and the elongation($\varepsilon_T$) at break is also significantly enhanced. In addition, the compressive strength($\sigma_c$) and compressive modulus ($E_c$) are also improved prominently. The strong H-bonding between PVA and HA, and the good dispersibility of HA endow the hydrogels with high modulus. The amorphous structure and the easy breakage of H-bonding provide the gels with an effective energy-dissipating mechanism, leading to their high tensile and compression strengths.

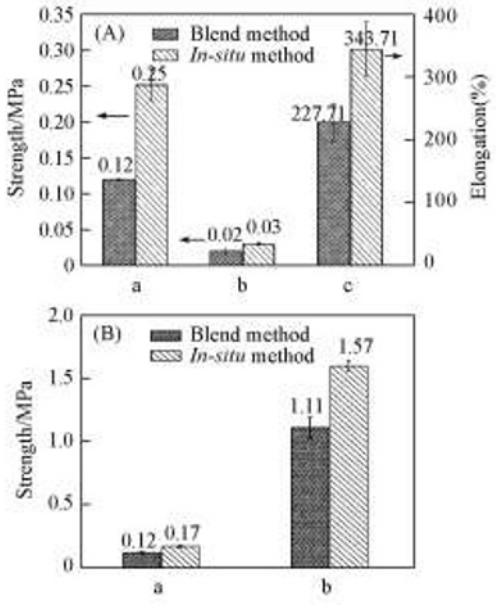


**Fig.4 Tensile(A) and compressive(B) properties of PVA/HA composite hydrogel prepared by blend method and *in-situ* method**

(A) a. $\sigma_T$; b. $E_T$; c. $\varepsilon_T$; (B) a. $\sigma_c$; b. $E_c$.

## 3.2 Formation Mechanism of PVA/HA Synthesized by *In-situ* Method

As shown in Fig.5, during the process of *in-situ* synthesis, on the one hand, $CaOH^+$ was formed by $Ca(OH)_2$ partly dissolved in water, which might interact with protonated hydroxyls of PVA through the oxygen lone pairs. On the other hand, hydroxyl group in $Ca(OH)_2$ and the free —OH in PVA molecules were linked by the forms of hydrogen bond. These two interactions promoted the $Ca(OH)_2$ distribution among inter- or intra-PVA molecular chains evenly, and the nucleation, growth and dispersion of HA in the PVA matrix[33]. The $Ca^{2+}$ cation in the HA and PVA molecule formed bond bridge band after HA formed, which improved the rigidity of composite hydrogel. Similarly, the hydrogen bonding between HA and PVA made them interlinked[34]. The high polar interactions in the macromolecular network system were caused when the pH value was adjusted to 10, which helped to form an infinite network of directional interactions or tie points that caused hydrogen bonding, enhancing the crystallinity of PVA hydrogel after cyclic F/T[35]. This will also increase the overall hydroxyl concentration and reduce the effectiveness of —OH as nucleation sites for HA crystals, promoting the uniform dispersion of HA in the PVA matrix[18]. What's more, the free motion of the PVA chain was restricted under freezing conditions, and that there is a greater possibility of hydrogen bonding between the molecular chains. The interaction forces in the system enhanced gradually with the increase of F/T cycle times. The strong coordination bonding and H-bonding between PVA and HA and the H-bonding between PVA molecular chains forced the formation of PVA/HA composite hydrogel, which enhanced the strength of the PVA/HA composites network.

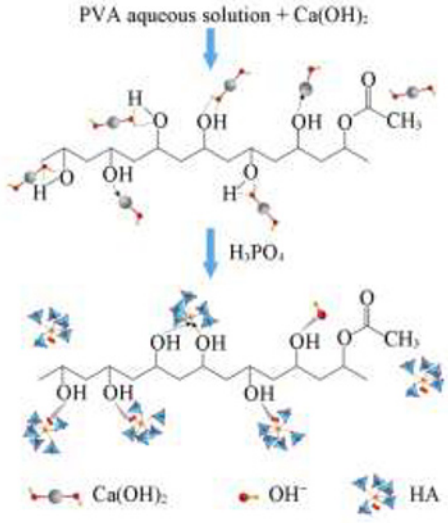


**Fig.5 Mechanism of the PVA/HA composite hydrogel prepared by *in-situ* method**

### 3.3 Influence of PVA Content on the PVA/HA Composite Hydrogel

The composite hydrogel with PVA mass fractions of 4%, 8%, 12% and HA mass fraction of 2% were prepared by *in-situ* synthesis method. The whole mixture solutions were homogeneous before freezing. Compared with the colorless transparent PVA aqueous solution, the composite solution presented uniformly white. After three F/T cycles, PVA/HA composite solution turned into white and elastic gel. In the preparation process, the PVA molecular chains intertwined and connected, which are retained after cyclic F/T, and formed the PVA semi-crystalline[36]. Fig.6 shows the XRD patterns of the PVA and PVA/HA composite hydrogel samples. It can be deduced that HA is located in the PVA matrix. However, the characteristic peak intensities of PVA were enhanced and the peaks intensities corresponding to HA were slightly decreased with the increase of PVA content.

SEM images of PVA/HA hydrogel with different PVA concentration are shown in Fig.7. The PVA/HA composite hydrogel presents a three-dimensional network structure as a whole. The increase of PVA content promotes the crystallization, and the skeleton thickens. And the size of porous structure increases accordingly. EDS analysis of 12%PVA/2%HA composite hydrogels was carried out to prove that the particles in the PVA matrix were HA. From Fig.8, it can be clearly observed the presence of calcium and phosphorous. Combined with other test results, it can be proved that HA is evenly distributed in the PVA gel system. With the increase of PVA content, the skeleton structure thickens gradually.

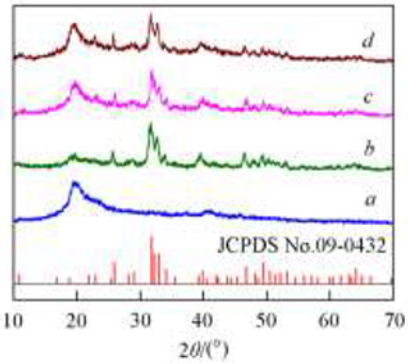


**Fig.6 XRD patterns of PVA hydrogel(*a*) and *x*%PVA/2%HA composite hydrogels(*b*—*d*)**

Mass fraction of PVA(*x*, %): *b*. 4; *c*. 8; *d*. 12.

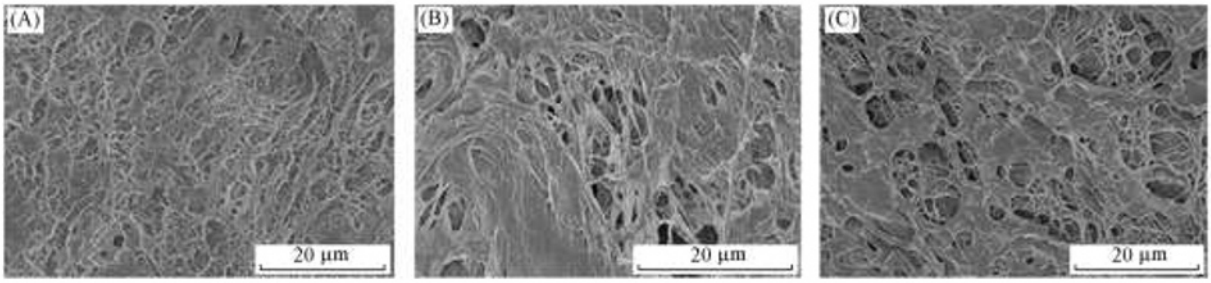


**Fig.7 SEM images of *x*%PVA/2%HA composite hydrogels**

Mass fraction of PVA(*x*, %): (A) 4; (B) 8; (C) 12.

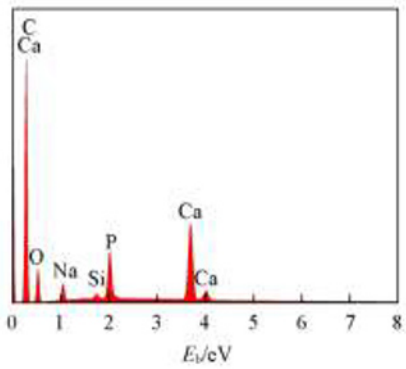


**Fig.8 EDS of PVA/HA composite hydrogel**

The tensile performance test results of PVA/HA composite hydrogel with different PVA concentration are shown in Fig.9(A). The increase of PVA content can improve the tensile strength and elastic modulus. When the content of PVA attains 12%, the tensile strength is 0.53 MPa, the breaking elongation accomplishes 272.40% and elastic modulus comes up to 0.10 MPa. The polymer structure and containing liquid would affect the behaviors of hydrogel under the external force[13]. Through the cyclic F/T, the three-dimensional network is filled with aqueous solutions. The PVA molecular chain and the

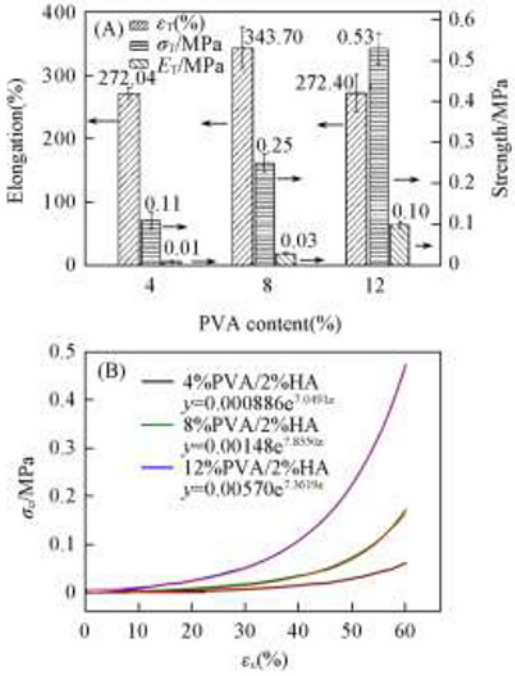


**Fig.9 Tensile(A) and compressive(B) properties of *x*%PVA/2%HA composite hydrogels**

unique network structure will adjust to the external forces along its direction. The interaction, crosslinking and friction in the system provide the gels a valid energy-dissipating mechanism, leading to their high tensile strengths and elongations[37,38].

The cylindrical samples were compressed to 40% to explore compressive property of composite hydrogels. Fig.9(B) shows the typical compressive stress-strain curves of the composite hydrogels prepared with different PVA contents. The curves fit an exponential function, with a correlation coefficient $R^2$ of more than 0.99 through the Origin 8.0 simulation. It can be seen that the increasing content of HA could improve the compressive property of the hydrogels. The special structure endows PVA/HA composite hydrogel good viscoelasticity[39]. PVA/HA composite hydrogels are made up of amorphous regions formed by PVA molecular chains, microcrystals formed by PVA molecular/inter-hydrogen bonding, HA nanoparticles and free water in three-dimensional network structures[40]. The three-dimensional net structure provides a lot of free space, making the polymer molecular chain rearrange when it responses to the external stimulus, concomitantly free water overflowing. The inner stresses make the composite hydrogels have good compressive properties. In addition, under the same strain value, the stress of PVA/HA hydrogel heightens with the increase of PVA content. For instance, when the strain is 60%, the compressive stress of the hydrogel rises from 0.06 MPa to 0.38 MPa, and the elastic modulus increases from 0.48 MPa to 2.91 MPa. The augment of PVA content increases the number and intensity of hydrogen bonds in the system, improving the tensile and compression performance[14].

### 3.4 Influence of HA Content on the PVA/HA Composite Hydrogel

8%PVA/*x*%HA composite hydrogels(*x*=1, 2, 3, 4, 6, 8) were *in-situ* prepared respectively. The SEM images are shown in Fig.10. Compared to pure 8%PVA hydrogel with a dense and microporous structure[as shown in Fig.2(B)], the composite hydrogels present crosslinking skeleton and interlacedly reticular structure with HA particles dispersing uniformly in the PVA matrix. When the content of HA increased to 2%, the reticular structure became more obvious. The skeleton structures augment are significantly wrapped around the network structure with the further increase of the content. As the HA mass fraction rises to 6%, the crosslinking skeleton structure becomes the main component. The reticular structures are separated from the crosslinked skeleton, and the HA granules aggregated[as shown in Fig.10(F)] in the PVA matrix when the HA content increased to 8%.

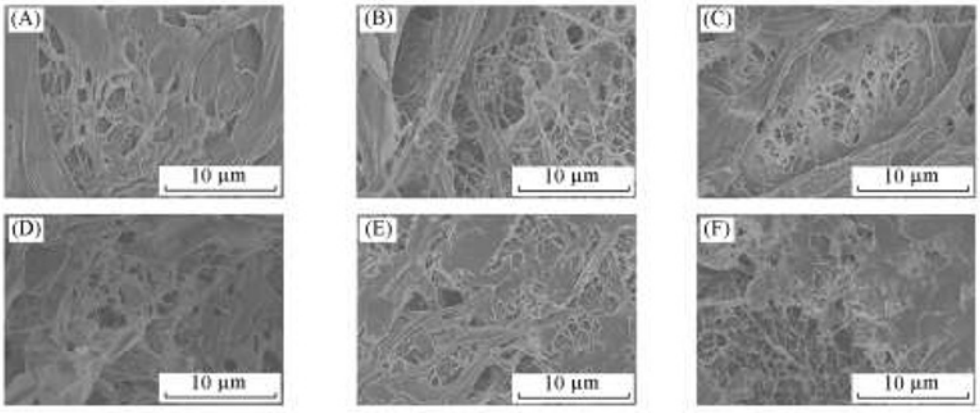


**Fig.10 SEM images of 8%PVA/*x*%HA composite hydrogels**

Mass fraction of HA(*x*, %): (A) 1; (B) 2; (C) 3; (D) 4; (E) 6; (F) 8.

The three-dimensional network structure of PVA/HA composite hydrogel is filled with solvents. Small molecular solvents can flow in and out of the porous structure, the water-absorbing swelling and shrinkage properties emerged. The PVA molecular chain contains a large number of hydrophilic hydroxyl groups. After cyclic F/T, solvent water is bound in the pores, making the composite hydrogel have a high moisture content, as shown in the Fig.11(A). The increase of HA content would thicken the PVA skeleton and reduce the pore structure, decreasing the water content. The number and thickness of the network structure determine the water absorption capacity of the composite hydrogels[41]. The increase of HA content

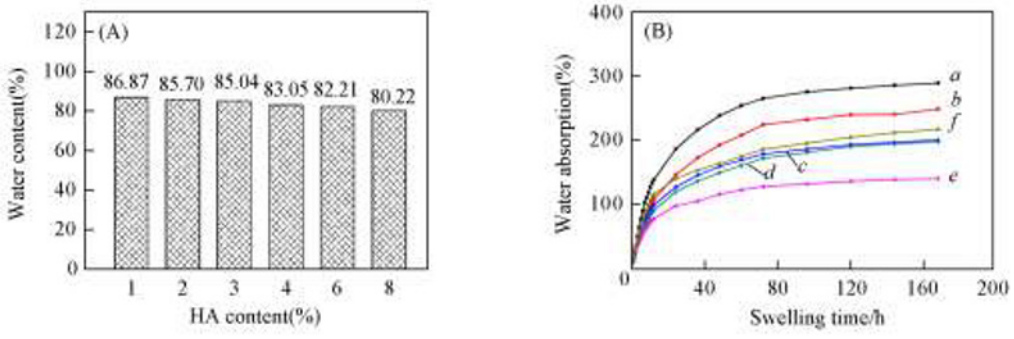


**Fig.11 Water content(A) and water absorption(B) of 8%PVA/*x*%HA composite hydrogels with different HA contents**

(A) Dry time: 60 h; drying temperature: 60 °C. (B) Swelling at 25 °C. Mass fraction of HA(*x*, %): *a*. 1; *b*. 2; *c*. 3; *d*. 4; *e*. 6; *f*. 8.

reduces the composite hydrogels' water absorption capacity. When the HA content is increased to 8%, the HA granules are aggregated in the PVA matrix, and the phase separation makes the water absorption raised.

The effect of HA content on the tensile and compressive properties of the composite hydrogel has been tested in Fig.12. In combination with the standard deviation, the tensile strength of composite hydrogel shows a slowly upward trend in general. The introduction of HA affects not only the strength of the hydrogel, but also its deformability. Therefore, the change trend of elastic modulus of hydrogel with different HA content was obtained by combining these two results, namely, the elastic modulus increases first and then decreases with the increase of HA content. It is demonstrated that the tensile resistance property of composite hydrogel with three F/T cycles and HA content of 6% is the best with tensile strength being 0.29 MPa, elasticity modulus being 0.12 MPa, and elongation being 200.98%. The mechanical properties of the composite hydrogel are expected to be improved effectively by adding HA nanoparticles into polymer matrix due to its high mechanical strength and surface energy[42]. The HA grows uniformly in the PVA matrix, which can significantly enhance the internal force of the system. Inversely, the HA particles can easily agglomerate due to its high surface active energy when the HA content reaches a certain value. The agglomeration of HA particles cannot act as a reinforcement phase but becoming the original defective region, which deteriorates the tensile strength of the composites[30]. As shown in Fig.10, when the HA content is higher than 6%, the HA particles appear to be agglomerated obviously, which will affect the mechanical properties. And the introduction of HA can also improve the compressive property of the composite hydrogel significantly, and the performance is the best when HA is 6%. When the compression ratio is 60%, its compressive strength increases to 0.40 MPa, and the compressive modulus is 2.99 MPa.

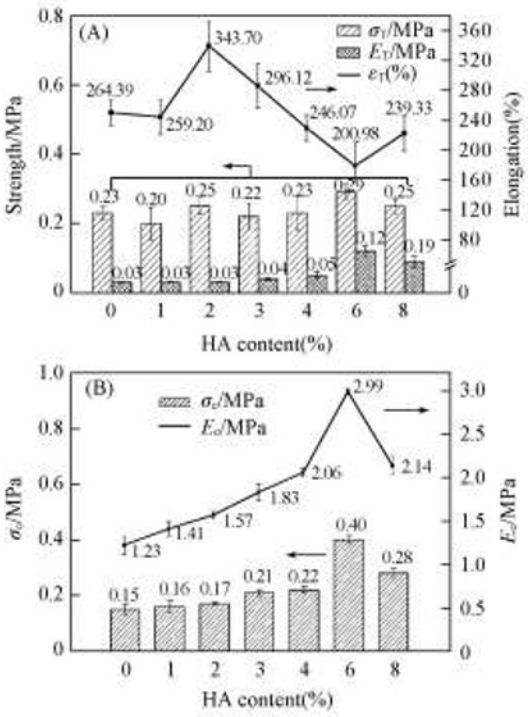


**Fig.12 Tensile(A) and compressive(B) properties of 8%PVA/*x*%HA composite hydrogels with pH value of 10**

## 3.5 Influence of pH on the PVA/HA Composite Hydrogel

For better application, we used the concentrated phosphoric acid to adjust the pH value of *in-situ* PVA/HA mixture to around 7 before cyclic F/T. From Fig.13, it can be found that the crystalline structure of the PVA and HA in PVA/HA composite hydrogel has not been changed after the pH value was adjusted to 7. Under the pH value of 10, phosphoric acid hydrolysis completely into phosphoric acid root, contributing to the formation and growth of HA crystal. After 4 h, the HA has been fully formed and combined with PVA very well. At this time the change of pH cannot affect the formation of HA crystals and the combination of PVA and HA.

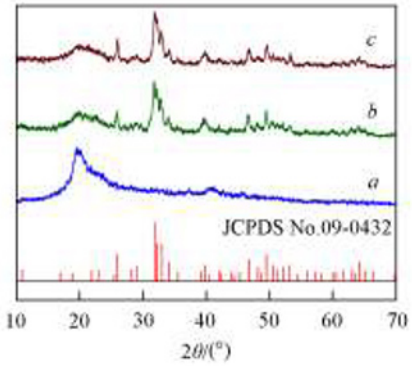


**Fig.13 XRD patterns PVA hydrogel(*a*) and PVA/HA composite hydrogels with pH of 10(*b*) and 7(*c*)**

The tensile and compressive properties of the composite hydrogel were also affected by the pH of the system(as shown in Fig.14). It can be observed that the tensile stress and strain

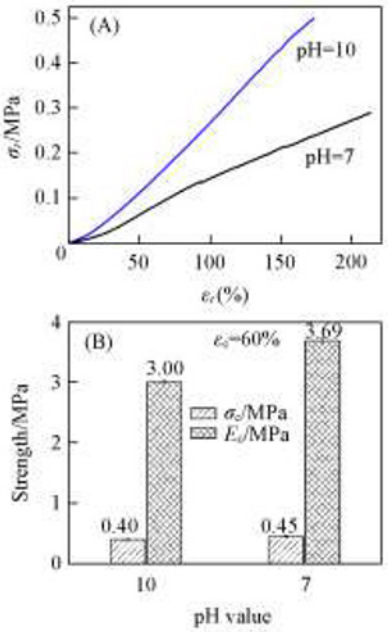


**Fig.14 Tensile(A) and compressive(B) properties of 8%PVA/6%HA composite hydrogel with different pH values**

curves assume a typical nonlinear tendency. Contrasted to the previous test results, the tensile properties of composite hydrogel were improved when the pH was adjusted to 7. As shown in Table 1, the tensile stress and modulus were enhanced significantly, the tensile strength increased from 0.29 MPa to 0.50 MPa, and the elastic modulus increased from 0.12 MPa to 0.22 MPa. When the pH value of system is 10, the excess hydroxide will interact with PVA and HA, respectively, so that some points on the HA do not combine with PVA. It neutralizes the excess sodium hydroxide after pH adjusted to 7. Some of the positions occupied by hydroxyl group are released, which promotes the interaction between HA and PVA, thus improving its mechanical properties.

**Table 1 Tensile and compressive properties of PVA/HA composite hydrogels with pH of 10 and 7**

| Property | $\sigma$/MPa | | $\varepsilon$(%) | | $E$/MPa | |
|---|---|---|---|---|---|---|
| | pH=10 | pH=7 | pH=10 | pH=7 | pH=10 | pH=7 |
| Tensile property | 0.29 | 0.50 | 200.98 | 173.29 | 0.12 | 0.22 |
| Compressive property | 0.40 | 0.45 | 60 | 60 | 2.99 | 3.69 |

For compressive properties, the same variation trend exists after pH adjusted to 7. When the compression ratio is 60%, the compressive strength of the composite hydrogel increases from 0.40 MPa to 0.45 MPa. The introduction of concentrated phosphoric acid also increases the content of ions in the system, it will be conducive to the formation of intermolecular aggregations due to the salting-out effect, and can increase the hydrophobic interchain interactions[43]. The increase of the interaction of the molecular chain would thicken the PVA reticular skeleton structure, as shown in Fig.15. The enhancing interchain aggregations would serve as the crosslinked point in network[44]. The thicker PVA skeleton and the stronger force improve the tensile and compression properties of the composite hydrogel.

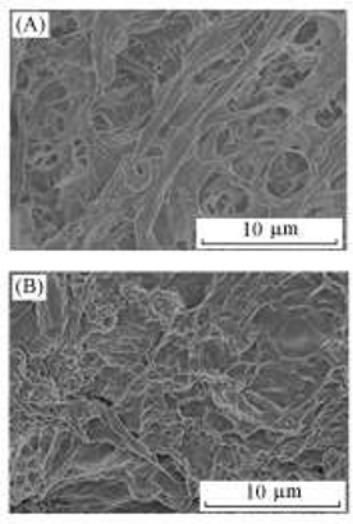


**Fig.15 SEM images of 8%PVA/6%HA composite hydrogel with pH of 10(A) and 7(B)**

## 4 Conclusions

In summary, we successfully *in-situ* prepared PVA/HA composite hydrogel through three cycles of freezing/thawing. Compared with simple blend, *in-situ* synthesis is more conducive to enhance the performance of the composite hydrogel. During the process of *in-situ* synthesis, the calcium forms the bond bridge band with the alcohol hydroxyl group in PVA and holds by Coulomb forces to ensure that $PO_4^{3-}$ could be combined with $Ca^{2+}$, initiating the nucleation, growth and dispersion of HA in the PVA matrix. The PVA/HA composite hydrogel presents a three-dimensional network structure, with the uniform distribution of HA nanoparticles. The reticular structure and strong force in the system make the PVA/HA composite hydrogels possess good tensile and compressive properties. In addition, pH value of the system is adjusted to 7 before freezing/thawing, which is not only beneficial to application but also can improve the mechanical properties of composite hydrogel.

## References

[1] Slaughter B. V., Khurshid S. S., Fisher O. Z., Khademhosseini A., Peppas N. A., *Advanced Materials*, **2009**, *21*(32/33), 3307
[2] Spiller K. L., Holloway J. L., Gribb M. E., Lowman A. M., *J. Tissue Eng. Regen. M*, **2011**, *5*(8), 636
[3] Zhang H. J., Xia H. S., Zhao Y., *ACS Macro Lett.*, **2012**, *1*(11), 1233
[4] Stammen J. A., Williams S., Ku D. N., Guldberg R. E., *Biomaterials*, **2001**, *22*(8), 799
[5] Kumar A., Han S. S., *Int. J. Polym. Mater. Po.*, **2017**, *66*(4), 159
[6] Kamoun E. A., Chen X., Eldin M. S. M., Kenawy E. R. S., *Arab. J. Chem.*, **2015**, *8*(1), 1
[7] Zhang L., Zhao J., Zhu J. T., He C. C., Wang H. L., *Soft Matter.*, **2012**, *8*(40), 10439
[8] Baker M. I., Walsh S. P., Schwartz Z., Boyan B. D., *J. Biomed. Mater. Res. B*, **2012**, *100B*(5), 1451
[9] Bhowmick S., Koul V., *Mat. Sci. Eng. C: Mater.*, **2016**, *59*, 109
[10] Moreau D., Villain A., Ku D. N., Corte L., *Biomatter*, **2014**, *4*, e28764
[11] Ferraz M. P., Monteiro F. J., Manuel C. M., *Journal of Applied Biomaterials & Biomechanics(JABB)*, **2004**, *2*(2), 74
[12] Xu F., Li Y., Wang X., Wei J., Yang A., *Journal of Materials Science*, **2004**, *39*(18), 5669
[13] Maiolo A. S., Amado M. N., Gonzalez J. S., Alvarez V. A., *Materials Science & Engineering C*, **2012**, *32*(6), 1490
[14] Li W., Wang D., Yang W., Song Y., *RSC Advances*, **2016**, *6*(24), 20166
[15] Sinha A., Das G., Sharma B. K., Roy R. P., Pramanick A. K., Nayar S., *Mat. Sci. Eng. C: Bio. S*, **2007**, *27*(1), 70
[16] Nayar S., Pramanick A. K., Sharma B. K., Das G., Kumar B. R., Sinha A., *J. Mater. Sci.-Mater. M*, **2008**, *19*(1), 301
[17] Pang Y. X., Bao X., *Journal of the European Ceramic Society*, **2003**, *23*(10), 1697
[18] Poursamar S. A., Rabiee M., Samadikuchaksaraei A., Tahriri M., Karimi M., Azami M., *J. Ceram. Process Res.*, **2009**, *10*(5), 679
[19] Sang S. B., Wu Q. M., Gan Z., *Electrochim. Acta*, **2008**, *53*(15), 5065
[20] Swain S. K., Bhattacharyya S., *Mat. Sci. Eng. C: Mater.*, **2013**, *33*(1), 67
[21] Pan Y. S., Xiong D. S., *J. Wuhan Univ. Technol.*, **2010**, *25*(3), 474
[22] Gupta S., Webster T. J., Sinha A., *J. Mater. Sci.-Mater. M*, **2011**,

*22*(7), 1763

[23] Paradossi G., Cavalieri F., Chiessi E., Spagnoli C., Cowman M. K., *J. Mater. Sci.-Mater. M*, **2003**, *14*(8), 687

[24] Gu Z. Q., Xiao J. M., Zhang X. H., *Bio-Medical Materials and Engineering*, **1998**, *8*(2), 75

[25] Sardinha V. M., Lima L. L., Belangero W. D., Zavaglia C. A., Bavaresco V. P., Gomes J. R., *Wear*, **2013**, *301*(1/2), 218

[26] Sinha A., Guha A., *Mat. Sci. Eng. C: Bio S.*, **2009**, *29*(4), 1330

[27] Hassan C. M., Peppas N. A., *Adv. Polym. Sci.*, **2000**, *153*, 37

[28] Mansur H. S., Orefice R. L., Mansur A. A. P., *Polymer*, **2004**, *45*(21), 7193

[29] Mansur H. S., Sadahira C. M., Souza A. N., Mansur A. A. P., *Mat. Sci. Eng. C: Bio. S*, **2008**, *28*(4), 539

[30] Gonzalez J. S., Alvarez V. A., *Journal of the Mechanical Behavior of Biomedical Materials*, **2014**, *34*, 47

[31] Lee Y. J., Lee G. H., Hwang J. S., Jeong S. W., Kim H. C., Kim E., Oh T. H., Lee S. J., Lee S. G., *Fiber Polym.*, **2016**, *17*(4), 502

[32] Tudorachi N., Chiriac A. P., *J. Polym. Environ.*, **2011**, *19*(2), 546

[33] Pan Y., Xiong D., *Journal of Materials Science Materials in Medicine*, **2009**, *20*(6), 1291

[34] Wei Q., Wang Y., Li X., Yang M., Chai W., Wang K., Zhang Y., *Journal of the Mechanical Behavior of Biomedical Materials*, **2016**, *57*, 190

[35] Nugent M. J. D., Hanley A., Tomkins P. T., Higginbotham C. L., *J. Mater. Sci.-Mater. M*, **2005**, *16*(12), 1149

[36] Chen Y. N., Peng L., Liu T., Wang Y., Shi S., Wang H., *ACS Applied Materials & Interfaces*, **2016**, *8*(40), 27199

[37] Ma R., Xiong D., Miao F., Zhang J., Peng Y., *Materials Science & Engineering C*, **2009**, *29*(6), 1979

[38] Zhang D. K., Wang D. G., Duan J. J., Ge S. R., *J. Bionic. Eng.*, **2009**, *6*(1), 22

[39] Pan Y. S., Xiong D. S., Gao F., *J. Mater. Sci.-Mater. M*, **2008**, *19*(5), 1963

[40] Ricciardi R., Auriemma F., Gaillet C., de Rosa C., Lauprêtre F., *Macromolecules*, **2004**, *37*(25), 9510

[41] Jin R., Teixeira L. S. M., Dijkstra P. J., Karperien M., Zhong Z., Feijen J., *J. Control. Release*, **2008**, *132*(3), E24

[42] Pan Y., Xiong D., Chen X., *Journal of Materials Science*, **2007**, *42*(13), 5129

[43] Yang Y., Wang X., Yang F., Shen H., Wu D., *Advanced Materials*, **2016**, *28*(33), 7178

[44] Sun Y., Xiang N., Jiang X., Hou L., *Materials Letters*, **2017**, *194*, 34